Dynamic Synchronization Between Multiple Cortical Motor Areas and Muscle Activity in Phasic Voluntary Movements

BERND FEIGE,[1] AD AERTSEN,[2] AND RUMYANA KRISTEVA-FEIGE[3]
[1]*Psychiatric Clinic and* [2]*Department of Neurobiology and Biophysics, Institute for Biology III, Albert-Ludwigs-University, D-79104 Freiburg; and* [3]*Neurological Clinic, Albert-Ludwigs-University, D-79106 Freiburg, Germany*

Received 27 March 2000; accepted in final form 1 June 2000

Feige, Bernd, Ad Aertsen, and Rumyana Kristeva-Feige. Dynamic synchronization between multiple cortical motor areas and muscle activity in phasic voluntary movements. *J Neurophysiol* 84: 2622–2629, 2000. To study the functional role of synchronized neuronal activity in the human motor system, we simultaneously recorded cortical activity by high-resolution electroencephalography (EEG) and electromyographic (EMG) activity of the activated muscle during a phasic voluntary movement in seven healthy subjects. Here, we present evidence for dynamic beta-range (16–28 Hz) synchronization between cortical activity and muscle activity, starting after termination of the movement. In the same time range, increased tonic activity in the activated muscle was found. During the movement execution a low-frequency (2–14 Hz) synchronization was found. Using a novel analysis, phase-reference analysis, we were able to extract the EMG-coherent EEG maps for both, low- and high-frequency beta range synchronization. The electrical source reconstruction of the EMG-coherent EEG maps was performed with respect to the individual brain morphology from magnetic resonance imaging (MRI) using a distributed source model (cortical current density analysis) and a realistic head model. The generators of the beta-range synchronization were not only located in the primary motor area, but also in premotor areas. The generators of the low-frequency synchronization were also located in the primary motor and in premotor areas, but with additional participation of the medial premotor area. These findings suggest that the dynamic beta-range synchronization between multiple cortical areas and activated muscles reflects the transition of the collective motor network into a new equilibrium state, possibly related to higher demands on attention, while the low-frequency synchronization is related to the movement execution.

INTRODUCTION

Synchronization between distributed neuronal activity patterns on a fine temporal scale has been proposed as a candidate mechanism for integration in the visual system (Eckhorn et al. 1988; Engel et al. 1992; Gray and Singer 1989; Singer and Gray 1995), in frontal areas (Abeles et al. 1993a,b; Prut et al. 1998), and in the visuomotor areas (Roelfsema et al. 1997). Little, however, is known about synchronization processes in the motor system (Baker et al. 1999; Brown 2000; Farmer 1998). The coherence in the beta frequency range observed in the human motor system between the electromyogram (EMG) and cortical activity measured by the magnetoencephalogram (MEG) (Conway et al. 1995; Salenius et al. 1997) or electroencephalogram (EEG) (Halliday et al. 1998; Mima et al. 2000) during sustained voluntary muscle contraction was interpreted as a sign of neural coordination, similar to the synchronization observed in monkeys (Baker et al. 1997; Murthy and Fetz 1992, 1996; Riehle et al. 1997; Sanes and Donoghue 1993). These studies (Conway et al. 1995; Halliday et al. 1998; Mima et al. 2000; Salenius et al. 1997) investigated the synchronization between human cortical activity and EMG of the active muscle during maintained isometric muscle contraction. Conway et al. (1995) and Salenius et al. (1997) found the coherence largely confined to cortical activity in the beta-range (15–30 Hz). They hypothesized that this coherence might reflect binding between synchronized cortical activity in the primary motor areas and motor output at the spinal level. Since these studies used a maintained muscle contraction task, it was impossible to assess the dynamical properties of the synchronization. Another open question is the localization of the sources of cortical synchronization. Both MEG studies located the generators of the beta synchronization in the primary motor cortex. However, since MEG recordings are only sensitive to tangential current components of active neuronal populations (Williamson and Kaufman 1981), as is the case in the primary motor area, possible contributions from sources having mostly radial components, such as in the premotor area (PMA), may have been overlooked (Kristeva et al. 1991). The two studies aiming at investigating the EEG/EMG synchronization (Halliday et al. 1998; Mima et al. 2000) were not able to locate such sources, due to the lack of spatial resolution with only two electrodes overlying the contralateral hand area (Halliday et al. 1998) or because no source reconstruction technique was applied (Mima et al. 2000).

To study whether beta-range and other synchronization between cortical activity and EMG in the human motor system also occurs under dynamic conditions and, if so, to examine the spectro-temporal properties of this synchronization and its relation to the onset and offset of muscle contraction, we employed a phasic motor task. Subjects performed a voluntary right index finger movement every 12–25 s [Bereitschaftspotential paradigm (Kornhuber and Deecke 1965)]. We simultaneously recorded the cortical activity by high-resolution EEG and the EMG of one of the activated muscles (the prime mover; Fig. 1). Since the EEG is sensitive to tangential as well as to

Address for reprint requests: R. Kristeva-Feige, Neurological Clinic, Albert-Ludwigs-University, Breisacher Straße 64, D-79106 Freiburg, Germany (E-mail: kristeva@nz11.ukl.uni-freiburg.de).

The costs of publication of this article were defrayed in part by the payment of page charges. The article must therefore be hereby marked "*advertisement*" in accordance with 18 U.S.C. Section 1734 solely to indicate this fact.

 0022-3077/00 $5.00 Copyright © 2000 The American Physiological Society

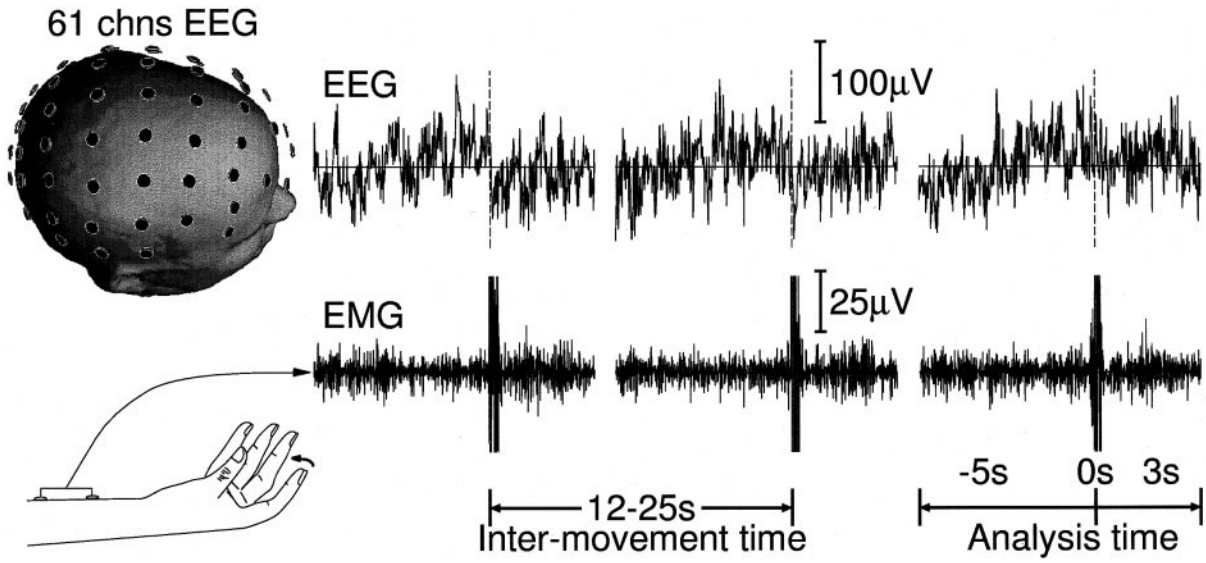

FIG. 1. Experimental paradigm. Electrode layout for 61 scalp electrodes superimposed on the digitized head contour for one of the subjects (*top left*). The *bottom left panel* illustrates the movement investigated. The electroencephalogram (EEG) from the C3 electrode, overlying the contralateral primary motor cortex, is shown for 3 consecutive movement-related EEG trials (*top right*). The *bottom right panel* illustrates the EMG recorded from m. flexor digitorum for 3 movement-related trials (for more details, cf. METHODS). The movement onset is marked by a dotted line.

radial sources, we could test whether other cortical areas besides the primary motor cortex become engaged in the synchronization between cortical activity and EMG. Moreover, the combination of a dynamic task paradigm and EEG recordings also allowed us to address another important issue in the study of motor control: the relation between the cortico-EMG synchronization and movement-related spectral power changes in the EEG/MEG. It is well known that a phasic voluntary movement is preceded by cortical desynchronization mostly in the mu-frequency range (10–13 Hz), whereas it is followed by postmovement synchronization mostly in the beta-range (15–30 Hz) (Feige 1999; Feige et al. 1996; Pfurtscheller 1992; Salmelin and Hari 1994). The question whether this excess postmovement beta-activity is actually synchronized with the EMG has not yet been addressed in other studies.

METHODS

Subjects

The experiment was run with seven healthy, right-handed subjects (mean age 28.2 ± 3.2 yr): six males and one female (*S3*), who had previously given their informed consent.

Experimental paradigm

During the experimental session, subjects were sitting in an electrically shielded, dimly lit room and performed abrupt, self-paced "pulse" movements (rapid flexion followed by extension of the right index finger), starting from light extension position, at irregular intervals of 12–25 s (cf. Fig. 1). They were instructed to be completely relaxed and to avoid any other movement and to fix their gaze on a light-emitting diode in front of them. The subjects were instructed to pay attention to finish the rapid pulse movement in the same position, from which the movement had started. Each subject was given several practice trials prior to the experiment until they reached a consistent EMG pattern for the pulse movement. Electric potentials were recorded from 61 electrode positions equally distributed over both hemispheres on the scalp (band-pass 0–100 Hz; sampling rate 500 Hz; NeuroScan, Herndon, VA). Electrode Cz was used as common recording reference; the ground was on the forehead. The surface EMG was recorded using Ag-AgCl electrodes placed over the pars indicis of the right flexor digitorum muscle (one of the prime mover muscles) and recorded with the same filters and sampling rate as the EEG. The low frequencies were included to investigate whether there was also a low-frequency synchronization between EEG and EMG. The EMG onset was used as a trigger for further analysis. The electro-oculogram (EOG) was recorded to exclude trials with eye movement artifacts. EEG, EMG, and EOG were digitally stored and analyzed off-line. The analysis time was set from 5 s before to 3 s after EMG-onset. Two hundred to 250 artifact-free trials per subject were used for further analysis. After each recording session, the electrode positions and the head contour of the subject were digitized using a three-dimensional (3-D) ultrasound localizing device (ZEBRIS).

Analysis of phase synchronization and phase reference analysis

The synchronization between the EEG and the EMG of the agonist muscle as a function of frequency and time was quantified by averaging the complex difference phase factors $e^{-i(\varphi EEG-\varphi EMG)}$ representing the phase difference between EEG and EMG in every single trial. The amplitude c of the resulting average represents a measure of the nonuniformity of the distribution of phase differences, i.e., a measure of *phase coherence* between the EEG and EMG, by means of the Rayleigh test (cf. Lütkenhöner 1991; Mardia 1972; we used Rayleigh's asymptotic formula for the probability distribution given by Strutt 1905, cited after Greenwood and Durand 1955). Therefore in the following, c will be called *phase coherence*. The statistical significance of the phase coherence c determined from N trials can then be calculated as $e^{-N\cdot c^2}$. Note that the usual definition of coherence includes amplitude covariation in addition to the stability of phase difference and corresponds to the square of this value in the case of constant amplitudes (cf. Bendat and Piersol 1971; Whalen 1971).

To localize the sources of EMG-coherent EEG activity, we employed a new variant of this phase coherence analysis: phase reference analysis (Feige 1999): if $a(f)$ is the complex Fourier coefficient at frequency f, we have $a(f) = |a(f)|e^{-i\varphi}$. For each frequency, the difference phase factor is multiplied with the corre-

sponding spectral EEG amplitude and then averaged across trials: $|a_{EEG}(f)|e^{-I[\varphi EEG(f)-\varphi EMG(f)]}$. The EMG thereby acts as a phase reference: its phase is subtracted from the EEG phase, while the EEG amplitude is retained. Thus phase reference analysis measures the fraction of the EEG that is reliably synchronized to the EMG. Since this measure, unlike conventional coherence analysis, preserves both amplitude and phase information of the EEG, the sources of EMG-coherent EEG activity can be localized by applying source reconstruction methods to the scalp distributions (or maps) of the extracted EMG-coherent electrical potentials.

Electric source reconstruction

Source reconstruction of the EMG-coherent EEG maps was performed on the basis of the individual brain morphology as obtained from MRI. To establish the spatial relationship between the electrode positions and the MRI, the digitized head contour was matched with the head-contour as obtained from MRI by means of a surface-matching algorithm (Huppertz et al. 1998). For structural MRI, the 3-D dataset with full head coverage and 1 mm^3 voxels was acquired using a volume-encoded fast low angle shot pulse sequence (FLASH) with TR/TE/alpha = 40 ms/60 ms/40°. The source reconstruction was performed using cortical current density analysis (CCD) (Ilmoniemi 1991; Wagner 1998). The CCD maps obtained in this way show the current flow distribution on the cortex, which can account for the potentials measured on the head surface. The ambiguity in the CCD model was removed by the "*minimum norm constraint*." This constraint uses a model term that is proportional to the square of the strength of the reconstructed currents. The regularization parameter was determined according to the χ^2-criterion. No assumptions about the number and location of cortical sources were made, except that all sources were constrained to a surface representing the cortical gray matter. For each individual subject, the segmented cortex with all individual gyri and sulci at about 50,000 sampled locations was used. To account for the shapes of liquor, skull and scalp, a realistic three-compartment Boundary Element Method model was used as the volume conductor head model. Only sources with at least 75% of the strength at the maximum current density itself were considered. Under these circumstances (sensor distribution, source model used, and color scale) the drop from 100 to 75% happens within a volume of 3 × 3 × 3 cm (Fuchs et al. 1999). Image segmentation, volume conductor modeling, source reconstruction, and visualization were performed using the CURRY software (CURRY 3.0, Philips Research, Hamburg, Germany).

RESULTS

Since movement-related EEG rhythms occurring at fixed locations and in a defined functional situation can have a broad or a narrow spectrum, depending on the subject (Feige et al. 1996), we examined for each individual subject the entire frequency range between 0 and 45 Hz over a time window running from 5 s before to 3 s after EMG onset (Fig. 2). This *frequency* × *time* plane approach differs from the conventional method of examining only the data filtered in the most responsive frequency bands (Pfurtscheller 1992; Salmelin and Hari 1994). The synchronization between the EEG and the EMG of the agonist muscle as a function of frequency and time was quantified by the phase coherence. Figure 2*A* shows the *frequency* × *time* distributions of EEG-EMG phase coherence for two (of 7) investigated subjects. To facilitate the interpretation, the movement-related *frequency* × *time* distributions of baseline-relative spectral power changes in EEG (Fig. 2*B*) and EMG (Fig. 2*C*) are shown for comparison. Observe that each subject exhibited two patches of EEG-EMG coherence with different spectro-temporal properties (Fig. 2*A*): an early, low-frequency coherence (demarcated by a dotted white frame) and a later, high-frequency coherence (solid white frame). The spectro-temporal properties of these two successive instances of EEG-EMG coherence for all seven investigated subjects are summarized in Table 1. The low-frequency coherence ranged from 2 to 14 Hz (with a maximum at 5 Hz) and started immediately after EMG onset. Probably, this low-frequency coherence between cortical activity and EMG represents a functional state of the oscillatory network related to the pulse movement execution. Following the movement, there is a functional change in the network state, characterized by the high-frequency coherence. This beta-range coherence lasted 1–2 s, ranged from 16 to 28 Hz (with a maximum between 19 and 24 Hz), and started after the "pulse" movement, which lasted approximately 400 ms. This coherent beta-range activity occurring after movement termination can, in fact, be observed in single trials, as is demonstrated in the three trials shown in Fig. 3. Note that coherent beta-range activity was present only after (Fig. 3*D*), but not before the movement (Fig. 3*C*). Interestingly, the increased tonic EMG after movement termination was not described in previous Bereitschaftspotential studies. Possibly, this activity is related to the active muscles reaching the new equilibrium state after conclusion of the active movement (Wachholder 1928).

The postmovement high-frequency coherence between cortical activity and EMG should be distinguished from the well-known postmovement cortical beta-synchronization that has been described extensively in the EEG (Pfurtscheller 1992) and MEG (Feige et al. 1996; Salmelin and Hari 1994) literature. This becomes apparent from a comparison between the *frequency* × *time* distributions of EEG-EMG phase coherence (Fig. 2*A*) and movement-related EEG spectral power differences (Fig. 2*B*). The EEG spectral power distributions indeed show the well-known cortical postmovement beta-synchronization, i.e., the elevation of beta-range EEG-power immediately after movement termination. In all subjects the area (in *frequency* × *time*) over which this elevation extends included the patch of EEG-EMG coherence (solid white frames in Fig. 2, *A* and *B*), but was distinctly larger (especially covering higher frequencies). Similarly, Fig. 2*C* demonstrates that also the EMG exhibits beta-range spectral power enhancement immediately after the voluntary movement. As in the EEG, this enhancement includes the spectral band of EEG-EMG coherence, but it is also distinctly broader, especially toward higher frequencies. Therefore only part of the spectral power enhancement known as postmovement beta-synchronization is actually coherent to part of the postmovement EMG.

To localize the cortical sources of EMG-coherent EEG activity, we employed a new variant of phase coherence analysis: phase reference analysis (Feige 1999) (cf. METHODS). Since this measure, unlike conventional coherence analysis, preserves both amplitude and phase information of the EEG, the sources of EMG-coherent EEG activity can be localized by applying source reconstruction methods to the scalp distributions (or maps) of the extracted EMG-coherent electrical potentials (Fig. 4*A*). Thus we reconstructed for all subjects the EMG-coherent EEG map at the maximum postmovement high-frequency coherence (i.e., the peak in the solid white frame in Fig. 2*A*) and at the maximum of the low-frequency coherence during the movement (i.e., the peak in the dotted white frame in Fig. 2*A*)

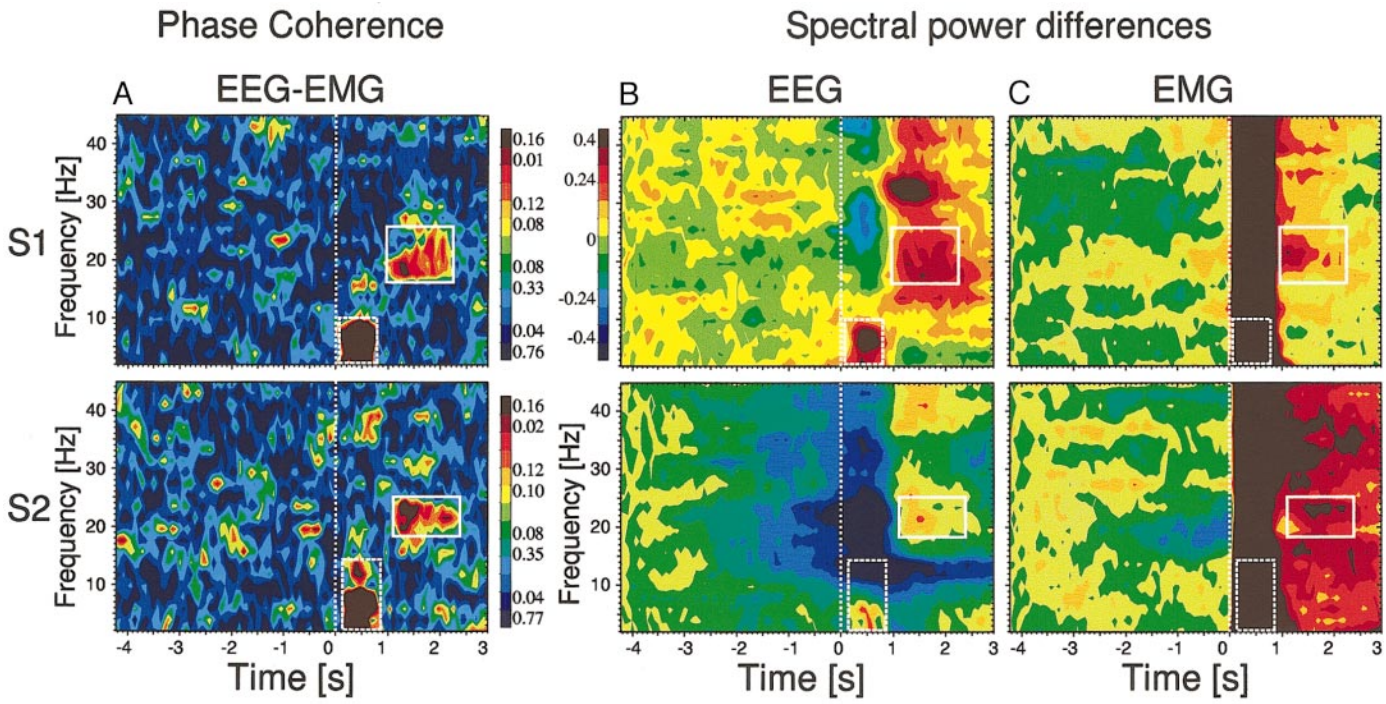

FIG. 2. Frequency × time plots of EEG-electromyographic (EMG) phase coherence (*A*) and movement-related EEG (*B*) and EMG (*C*) spectral power changes. Data, taken from repeated trials for 2 (of 7) subjects investigated. Time window from 5 s before to 3 s after EMG onset (vertical white dotted line at 0 ms). Phase coherence values were coded according to the shown color bars, with the values above indicating the phase coherence value, and the values below denoting the probability of observing this phase coherence by chance (Rayleigh test). The color bar for the spectral power changes applies to both subjects. Frequency analysis was performed using a sliding time window of width 768 ms, in which 2 512-ms fast Fourier transforms (FFTs) overlapping by half were calculated (for this reason, the figure only shows values starting at 4.2 s prior to the movement). The data in each FFT window were demeaned and detrended prior to FFT analysis. The resulting frequency resolution was 1.9 Hz. The analysis window was shifted in steps of 42 ms across each epoch for each of the channels. All reported latencies refer to the delay between EMG onset and the end of the analysis time window. *A*: movement-related *frequency* × *time* distributions of the EEG-EMG phase coherence. The EEG channel shown is the one with the maximum 16–28 Hz postmovement coherence with the EMG, as measured against common average reference. Observe that subjects exhibited 2 patches of strong EEG-EMG coherence (cf. Table 1): *1*) Low-frequency (2–14 Hz) coherence, starting immediately at EMG onset. This coherence (demarcated by a dotted white frame) most likely reflects the movement-related EEG potentials, found by EMG-onset triggered averaging of the EEG; they show up in the phase coherence analysis because the EMG-burst contains components of practically all frequencies, synchronized to movement onset (cf. *C*). *2*) High-frequency (23 ± 3 Hz) coherence, starting after the movement (which lasted approximately 400 ms) and peaking at 964 ± 283 ms after EMG onset. This high-frequency coherence (demarcated by a solid white frame) after a phasic voluntary movement was not previously described. The spectro-temporal properties and statistical significance of the 2 successive instances of movement-related EEG-EMG coherence for all 7 subjects are summarized in Table 1. *B*: *frequency* × *time* distributions of movement-related EEG spectral power changes, measured as the reliability of difference relative to a reference interval between 5 and 4 s before movement onset [relative gain G_r (Feige 1999; Feige et al. 1996)]. G_r is −1 for fully reliable power decrease, 0 for no change, and 1 for fully reliable power increase. Both subjects showed a clear increase in spectral power, covering a wide frequency range from 10–45 Hz (details depending on the subject), which started about 800 ms after EMG onset (i.e., beginning after movement termination). Note that the excess spectral power in the EEG, reflecting the well-known postmovement cortical beta-synchronization, includes the patch of beta-range EEG-EMG coherence, but covers a distinctly wider frequency range (cf. solid white frames, copied from *A*). *C*: movement-related *frequency* × *time* distributions of the EMG, computed in the same way as done for the EEG (*B*). The postmovement EEG/EMG synchronization (solid white frames, copied from *A*) occurred after termination of the movement-related EMG burst (dark vertical strip between 0 and 1 s). Observe, however, that the EMG spectral power does not return to baseline levels immediately, but exhibits a residual enhancement that (like the EEG) includes, but clearly extends beyond the beta-band EEG-EMG coherence.

by applying cortical current density analysis (cf. METHODS), using the individual brain anatomy derived from the subjects' magnetic resonance imaging (MRI). All seven subjects exhibited extended cortical current density sources for the high-frequency coherence comprising tangential activity in the contralateral primary motor cortex (cMI) but, in contrast to earlier reports, the extended source area included additional radial activity in the contralateral premotor area (cPMA; Fig. 4, *A* and *B*). Besides the tangential activity in MI and the radial activity in cPMA, in two of the subjects the source area included additional radial activity in the contralateral parietal area (cPA). In fact, never before were so many motor areas shown to engage in coherent activity so late after termination of an active movement. The finding that multiple motor areas are simultaneously involved is supported by the original high-frequency EMG-coherent EEG maps as shown for one of the subjects in Fig. 4*A*: the electric field distribution suggests contributions not only from a tangential source (within cMI) but also from a radial source (within the cPMA). This activation of multiple motor areas can be explicitly seen also in the tangential (cMI) and radial (cPMA) orientation of the individual current vectors (Fig. 4*B*). To compare the sources of the

TABLE 1. *Spectro-temporal properties of coherent population activity in motor cortical areas and EMG in relation to voluntary finger movements*

		EEG-EMG Coherence I: During Movement, Low-Frequency				EEG-EMG Coherence II: Post-Movement, High-Frequency			
Subject	Number of Trials	Latency, ms	Frequency, Hz	Maximal phase coherence	Significance, Rayleigh test	Latency, ms	Frequency, Hz	Maximal phase coherence	Significance, Rayleigh test
S1	171	20–750	2–10	0.476	$1.5 \cdot 10^{-17}$	1,000–2,200	16–26	0.182	$3.4 \cdot 10^{-3}$
S2	163	100–800	2–14	0.601	$2.7 \cdot 10^{-26}$	1,100–2,400	18–25	0.221	$3.6 \cdot 10^{-4}$
S3	100	100–650	2–8	0.498	$1.7 \cdot 10^{-11}$	1,450–2,300	22–25	0.144	0.12
S4	338	150–750	2–14	0.419	$1.7 \cdot 10^{-26}$	850–2,800	18–28	0.268	$2.8 \cdot 10^{-11}$
S5	246	75–800	2–12	0.602	$2.2 \cdot 10^{-39}$	800–2,100	20–25	0.141	$7.5 \cdot 10^{-3}$
S6	211	75–800	2–8	0.639	$3.9 \cdot 10^{-38}$	870–2,100	25–26	0.162	$3.5 \cdot 10^{-3}$
S7	272	150–900	2–8	0.616	$1.3 \cdot 10^{-45}$	1,535–1,900	23–25	0.098	0.07

The statistical significance P of a given coherence value c determined from N trials can be calculated as $e^{-N \cdot c^2}$, describing the probability of observing a phase coherence of this or larger amplitude by chance (Rayleigh test, using the asymptotic formula given by Strutt 1905). We used these phase coherence values in order to identify the latency and frequency ranges with the statistically most reliable EEG-EMG synchronization (cf. white dotted and solid frames in Fig. 2*A*). EEG, electroencephalogram; EMG, electromyogram.

beta-range coherence with those of the low-frequency coherence during the movement, a source reconstruction of the EMG-coherent EEG map at the maximum low-frequency coherence (i.e., the peak in the dotted white frame in Fig. 2*A*) was also performed. The reconstruction of the low-frequency coherence maps showed an extended source area including again the primary motor cortex and the premotor area (cf Fig. 4*D*). However, in the low-frequency EMG-coherent EEG maps, in addition more medial parts of the premotor area were engaged. The finding that the primary motor, premotor, and medial premotor areas are simultaneously involved is also supported by the complex pattern of the original EMG-coherent EEG maps shown in Fig. 4*C*.

DISCUSSION

The present results are the first to show that motor cortical areas and the EMG synchronize their joint activity in a dynamic fashion in systematic relation to phasic voluntary movements. Low-frequency (≈5 Hz) synchronization, starting at

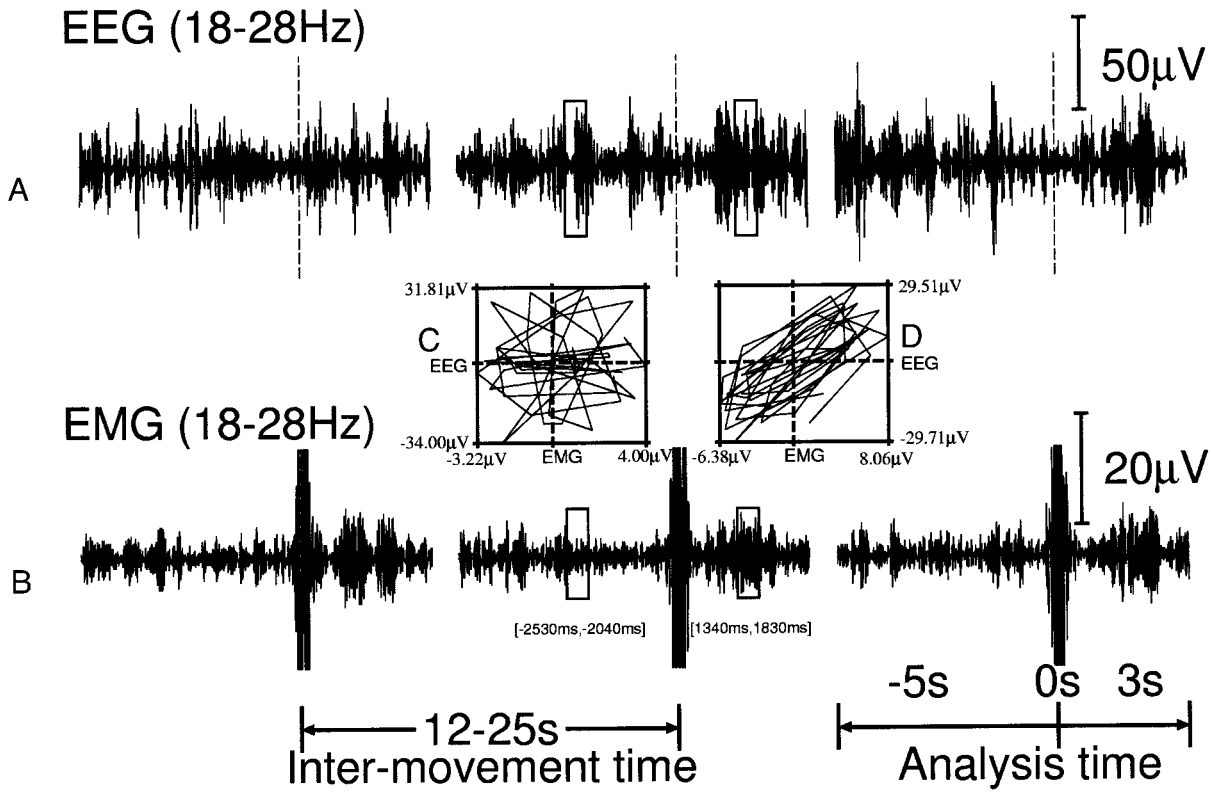

FIG. 3. EEG and EMG traces filtered in the beta-frequency range. The EEG (*A*) and EMG (*B*), filtered between 18 and 28 Hz, from the same 3 consecutive movement-related trials as shown in Fig. 1. The movement onset is marked by a dotted line. Note that short periods of enhanced beta-range activity in both EEG and EMG occurred during about 1 s after movement onset in each of the 3 trials. The insets (*C*) and (*D*) show the EEG and EMG signals plotted against each other for time intervals (indicated by frames) before and after the movement onset in the 2nd trial in *A* and *B*. Observe that there is no phase relationship between EEG and EMG in the premovement interval (*C*), whereas a clear phase relationship is present in the postmovement interval (*D*).

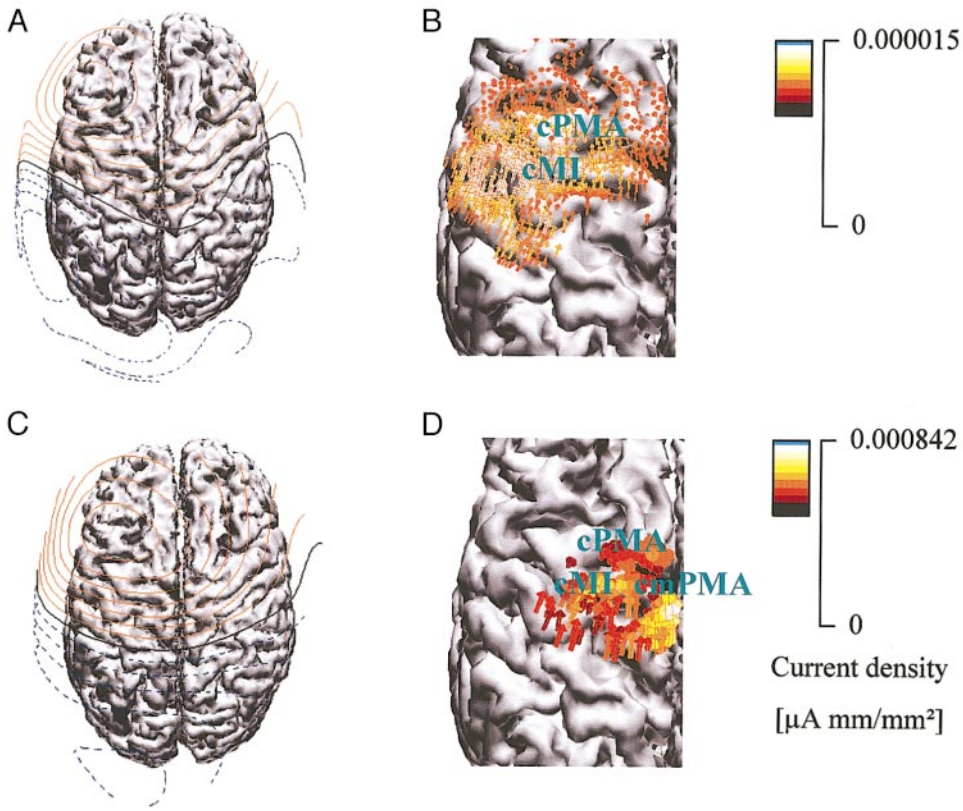

FIG. 4. Sources of the high- and low-frequency EMG-coherent EEG activity for one of the subjects. Top view of the MRI reconstruction of the cerebral cortex for this subject (nose pointing upward). CMI, contralateral primary motor area; cPMA, contralateral premotor area; cmPMA, contralateral medial premotor area. *A*: potential distribution of the high-frequency EMG-coherent EEG activity superimposed onto MRI reconstruction. Complex potential distribution pattern, suggesting activation of multiple areas. *B*: magnification of the reconstructed cortical current density (CCD) map underlying the potential distribution in *A*. The CCD map is displayed with individual current vectors. Scaling according to color bar. Extended CCD source in cMI and cPMA. The tangential currents are consistent with activation of the cMI in the anterior bank of the central sulcus; the radial currents are consistent with activation of the cPMA. *C*: potential distribution of the low-frequency EMG-coherent EEG activity superimposed onto MRI reconstruction. Complex potential distribution pattern, suggesting again activation of multiple areas. *D*: magnification of the reconstructed CCD map underlying the potential distribution in *C*. The CCD map is displayed with individual current vectors. Scaling according to color bar. Extended cortical current density source in cMI, cPMA, and cmPMA. The tangential currents are consistent with activation of the cMI in the anterior bank of the central sulcus, the radial currents are consistent with additional activation of the medial cPMA.

movement onset, is followed by high-frequency (≈23 Hz) synchronization after movement termination, lasting for 1–2 s. This synchronization dynamics may reflect changes in functional network state related to phasic voluntary movements. Beta-range synchronization between cortical activity and EMG had previously been observed during maintained motor tasks (Brown 2000; Conway et al. 1995; Halliday et al. 1998; Mima et al. 2000; Salenius et al. 1997), but never before under dynamic conditions with a phasic motor task. The close tuning of the EEG-EMG synchronization in all investigated subjects around ≈23 Hz, a frequency at which also coherence between human single motor unit spike trains was reported (Farmer et al. 1993), suggests that this may be a preferred frequency for integration of distributed activity in the motor system.

Comparison between the *frequency* × *time* distributions of EEG-EMG coherence (Fig. 2*A*) and movement-related EEG spectral power difference (Fig. 2*B*) revealed clear differences in the spectro-temporal extent of the two postmovement synchronization phenomena. This indicates that the postmovement beta-synchronization of the EEG/MEG, presumably reflecting the internal synchronization of relatively large cortical areas, is composed of at least two components: one that is coherent with the EMG (cf. Fig. 2*A*) and one that is not (the remainder). Moreover, the two components cover different frequency ranges. This finding that the postmovement cortical beta-synchronization is of a composite nature implies that the notion that it reflects idling motor cortex (Pfurtscheller 1992) or inhibition (Salmelin and Hari 1994) needs to be revised. Instead, it lends support to our earlier hypothesis that postmovement cortical beta-synchronization plays an active role in motor control, possibly integrating distributed activity between the cortex and the muscle (Brown 2000; Feige et al. 1996; Kilner et al. 1999).

The high-resolution EEG used in this study enabled us to localize generators of the beta-range EMG-synchronized cortical activity not only in the contralateral primary motor areas MI but also in the PMA. The contribution of the premotor areas to the generation of the EEG-EMG synchronization was overlooked in earlier MEG studies, presumably because the sensitivity of the MEG is restricted to tangential sources. The dynamic synchronization of the premotor areas and muscle activity may be important for postural stabilization after move-

ment. One possible mechanism for this may be related to the predominantly inhibitory action of premotor areas on pyramidal tract neurons as recently shown (Tokuno and Nambu 2000).

In all subjects we observed a joint participation of the contralateral MI area and the PMA. In two of the subjects, the contralateral PA engaged in the coherent EEG-EMG activation as well, suggesting the existence of inter-individual differences in the human motor system.

The contralateral primary motor and premotor areas were found to generate also the low-frequency cortico-EMG coherence during the voluntary movement. The activation of these two areas with the additional participation of the more medial parts of the premotor area may represent a functional state of the oscillatory motor network related to the movement execution.

It is interesting to note that the beta-range EEG/EMG synchronization occurred during the transition of the motor system into a new equilibrium state when the attentional demands of the motor tasks are higher because the subjects were instructed to pay special attention to finish the rapid pulse movement in the same position from which the movement has started. During this transition, there was an increased tonic activity in the active muscle (cf. Fig. 3*B*). Also Baker et al. (1997) and Kilner et al. (1999) presented evidence for beta-range cortico-EMG coherence during a stationary phase of a movement paradigm (a hold phase after a precision grip task), but not during active movement periods. Likewise, Conway et al. (1995), Salenius et al. (1997), and Halliday et al. (1998) demonstrated such coherent activity during maintained motor contraction and suggested that it might reflect a low-effort contraction maintenance rhythm. These findings suggest that the dynamic beta-range synchronization between multiple cortical areas and activated muscles reflects the transition of the collective motor network into a new equilibrium state, possibly related to higher demands on attention.

We thank Prof. C. H. Lücking for helpful discussions and C. Sick and T. Ball for experimental and analysis help. We are indebted to Drs. Leonardo Cohen, Bernhard Conway, Manfred Fuchs, Alexa Riehle, Jerome Sanes, Andrew Schwartz, and Mario Wiesendanger for constructive comments on an earlier version of the manuscript.

This work was supported in part by grants from the Deutsche Forschungsgemeinschaft and the Research Fund of the Albert-Ludwigs-University Freiburg.

REFERENCES

ABELES M, BERGMAN H, MARGALIT E, AND VAADIA E. Spatiotemporal firing patterns in the frontal cortex of behaving monkeys. *J Neurophysiol* 70: 1629–1643, 1993a.

ABELES M, PRUT Y, BERGMAN H, VAADIA E, AND AERTSEN A. In: *Brain Theory: Spatio-temporal Aspects of Brain Function,* edited by Aertsen A. New York: Elsevier, 1993b.

BAKER SN, KILNER JM, PINCHES EM, AND LEMON RN. The role of synchrony and oscillations in the motor output. *Exp Brain Res* 128: 109–117, 1999.

BAKER SN, OLIVIER N, AND LEMON RN. Coherent oscillations in monkey motor cortex and hand muscle EMG show task-dependent modulation. *J Physiol (Lond)* 501.1: 225–241, 1997.

BENDAT JS AND PIERSOL AG. *Random Data. Analysis and Measurement Procedures.* New York: Wiley, 1971.

BROWN P. Cortical drives to human muscle: the Piper and related rhythms. *Prog Neurobiol* 60: 97–108, 2000.

CONWAY BA, HALLIDAY DM, FARMER SF, SHAHANI U, MAAS P, WEIR AI, AND ROSENBERG JR. Synchronization between motor cortex and spinal motoneuronal pool during the performance of a maintained motor task in man. *J Physiol (Lond)* 489: 917–924, 1995.

ECKHORN R, BAUER R, JORDAN W, BROSCH M, KRUSE W, MUNK M, AND REITBOECK HJ Coherent oscillations: a mechanism of feature linking in the visual cortex? Multiple electrode and correlation analyses in the cat. *Biol Cybern* 60: 121–130, 1988.

ENGEL AK, KÖNIG P, KREITER AK, SCHILLEN TB, AND SINGER W. Temporal coding in the visual cortex: new vistas on integration in the nervous system. *Trends Neurosci* 15: 218–226, 1992.

FARMER SF. Rhythmicity, synchronization and binding in human and primate motor systems. *J Physiol (Lond)* 509.1: 3–14, 1998.

FARMER SF, BREMNER FD, HALLIDAY DM, ROSENBERG JR, AND STEPHENS JA. The frequency content of common synaptic inputs to motoneurones studied during voluntary isometric contraction in man. *J Physiol (Lond)* 470: 127–155, 1993.

FEIGE B. *Oscillatory Brain Activity and Its Analysis on the Basis of MEG and EEG*. New York: Waxmann, 1999.

FEIGE B, KRISTEVA-FEIGE R, ROSSI S, PIZZELLA V, AND ROSSINI PM. Neuromagnetic study of movement-related changes in rhythmic brain activity. *Brain Res* 734: 252–260, 1996.

FUCHS M, WAGNER M, KOHLER T, AND WISCHMANN HA. Linear and nonlinear current density reconstructions. *J Clin Neurophysiol* 16: 267–295, 1999.

GRAY CM AND SINGER W. Stimulus-specific neuronal oscillations in orientation columns of cat visual cortex. *Proc Natl Acad Sci USA* 86: 1698–1702, 1989.

GREENWOOD JA AND DURAND D. The distribution of length and components of the sum of n random unit vectors. *Ann Math Stat* 26: 233–246, 1955.

HALLIDAY DM, CONWAY BA, FARMER SF, AND ROSENBERG JR. Using electroencephalography to study functional coupling between cortical activity and electromyograms during voluntary contractions in humans. *Neurosci Lett* 241: 5–8, 1998.

HUPPERTZ JH, OTTE M, GRIMM C, KRISTEVA-FEIGE R, MERGNER T, AND LÜCKING CH. Estimation of the accuracy of a surface matching technique for registration of EEG and MRI data. *Electroencephalogr Clin Neurophysiol* 106: 409–415, 1998.

ILMONIEMI RJ. Estimates of neuronal current distributions. *Acta Oto-Laryngol Suppl* 491: 80–87, 1991.

KILNER JM, BAKER SN, SALENIUS S, JOUSMAKI V, HARI R, AND LEMON RN. Task-dependent modulation of 15–30 Hz coherence between rectified EMGs from human hand and forearm muscles. *J Physiol (Lond)* 516.2: 559–570, 1999.

KORNHUBER H AND DEECKE L. Hirnpotentialänderungen bei Willkürbewegungen und passiven Bewegungen des Menschen: Bereitschaftspotential und reafferente Potentiale. *Pflügers Arch* 284: 1–17, 1965.

KRISTEVA R, CHEYNE D, AND DEECKE L. Neuromagnetic fields accompanying unilateral and bilateral voluntary movements: topography and analysis of cortical sources. *Electroencephalogr Clin Neurophysiol* 81: 284–298, 1991.

LÜTKENHÖNER B. Theoretical considerations on the detection of evoked responses by means of the Rayleigh test. *Acta Otolaryngol (Stockh)* 491: 52–60, 1991.

MARDIA K. *Statistics of Directional Data.* New York: Academic, 1972.

MIMA T, STEGER J, SCHULMAN AE, GERLOFF CH, AND HALLETT M. Electroencephalographic measuremnent of motor cortex control of muscle activity in humans. *Clin Neurophysiol* 111: 326–337, 2000.

MURTHY VN AND FETZ EE. Coherent 25- to 35-Hz oscillations in the sensorimotor cortex of awake behaving monkeys. *Proc Natl Acad Sci USA* 89: 5670–5674, 1992.

MURTHY VN AND FETZ EE. Oscillatory activity in sensorimotor cortex of awake monkeys: synchronization of local field potentials and relation to behavior. *J Neurophysiol* 76: 3949–3967, 1996.

PFURTSCHELLER G. Event-related synchronization (ERS): an electrophysiological correlate of cortical areas at rest. *Electroencephalogr Clin Neurophysiol* 83: 62–69, 1992.

PRUT Y, VAADIA E, BERGMAN H, HAALMAN I, SLOVIN H, AND ABELES M. Spatiotemporal structure of cortical activity: properties and behavioral relevance. *J Neurophysiol* 79: 2857–2874, 1998.

RIEHLE A, GRÜN S, DIESMANN M, AND AERTSEN A. Spike synchronization and rate modulation differentially involved in motor cortical function. *Science* 278: 1950–1953, 1997.

ROELFSEMA PR, ENGEL A, KÖNIG P, AND SINGER W. Visuomotor integration is associated with zero time-lag synchronization among cortical areas. *Nature* 385: 157–161, 1997.

ROSENBERG JR, AMJAD AM, BREEZE P, BRILLINGER DR, AND HALLIDAY DM. The Fourier approach to the identification of functional coupling between neuronal spike trains. *Prog Biophys Mol Biol* 53: 1–31, 1989.

SALENIUS S, PORTIN K, KAJOLA M, SALMELIN R, AND HARI R. Cortical control of human motoneuron firing during isometric contraction. *J Neurophysiol* 77: 3401–3405, 1997.

SALMELIN R AND HARI R. Spatiotemporal characteristics of sensorimotor neuromagnetic rhythms related to thumb movement. *Neuroscience* 60: 537–550, 1994.

SANES JN AND DONOGHUE JP. Oscillations in local field potentials of the primate motor cortex during voluntary movement. *Proc Natl Acad Sci USA* 90: 4470–4474, 1993.

SINGER W AND GRAY CM. Visual feature integration and the temporal correlation hypothesis. *Annu Rev Neurosci* 18: 555–586, 1995.

STRUTT JW. The problem of the random walk. *Nature* 72: 318, 1905.

TOKUNO H AND NAMBU A. Organization of nonprimary motor cortical inputs on paramidal and nonpyramidal tract neurons of primary motor cortex: an electrophysiological study in the macaque monkey. *Cereb Cortex* 10: 58–68, 2000.

WACHHOLDER K. *Willkürliche Haltung und Bewegung. Ergebnisse der Physiologie.* Munich, Germany: Von J. F. Bergmann, 1928, p. 568–645.

WAGNER M. *Rekonstruktion neuronaler Ströme aus bioelektrischen und biomagnetischen Messungen auf der aus MR-Bildern segmentierten Hirnrinde.* Aachen, Germany: Shaker Verlag, 1998.

WHALEN AD. *Detection of Signals in Noise*. New York: Electrical Science, Academic, 1971.

WILLIAMSON SJ AND KAUFMAN L. Biomagnetism. *J Magn Magn Mat* 22: 129–201, 1981.